Journal of Data Acquisition and Processing
ISSN: 1004-9037
https://sjcjycl.cn/
DOI: 10.5281/zenodo.754683

FACIAL KEY POINTS AND CONTOUR IDENTIFICATION FOR FACIAL PARALYSIS IMAGES

Samuel Susan Veeravalli
Dept. of Computer Science and Systems Engineering, Andhra University, Visakhapatnam, India, vssusan.rs@andhrauniversity.edu.in

Dr. Prajna Bodapati
Dept. of Computer Science and Systems Engineering, Andhra University, Visakhapatnam, India, prof.bprajna@andhrauniveristy.edu.in

Abstract – Facial Paralysis is one of the neural disorders that is increasing nowadays. Anyone can be infected by this when the cranial nerve is affected. As a result, they will not be able to contract the muscles on the face on either of the sides. This directly affects the social life of patients who has this palsy, as they couldn't show much expression and communicate naturally like other healthy persons. Computer vision-based algorithms that are based on the CNN model and auto encoders can be used for accurate identification with precision and allow the extraction of high-level information from these facial key points, so that detection of facial paralysis can be used for the betterment of medical diagnosis. In this paper, the MediaPipe framework is used to identify the necessary key points of the facial parts of images containing palsy. The framework provides the key points for entire face which are used in many applications like a face mesh, among those the essential points are the facial parts which are required for analysis of palsy are considered.

Keywords—Facial key points, contours, palsy, MediaPipe.

I. INTRODUCTION

Facial paralysis is a weakness or damage caused to the facial nerve that disables the regular movement of muscles in face, although this is not so commonly seen in individuals earlier, in recent times the rate of this illness is increasing in present world. According to a study in [1], with the increase in population nowadays the occurrence of the paralysis is about 30 out of 100,000 persons. Facial palsy is also called as facial nerve paralysis can be temporary or permanent effect on face. As the muscles in the face cannot get the necessary signal for normal functioning it results in paralyzed portion on the face, making the movement of eyes, lips and other parts difficult. A person who is infected with facial paralysis may suffer with difficulty in performing normal actions like blinking of eyes, expressions, swallowing, etc. This directly effects the social life of them as it leaves the face with asymmetry and to express themselves in their regular life. Facial paralysis can also appear in different degree among people irrespective of age, gender or previous health conditions. It also affects total face or a part of the face like lower part of face or on either side of the face. The asymmetry might be because the facial nerve on that side gets damaged, and the cranial nerve which is present on the sides of the face are independent with their functionality. The brain is the origin of the nerve and passes through the face and split into five branches in front of the ears. The facial expressions

are created with these muscles from these branches. The other controls of the facial nerve are taste, tears and salivation.

Facial paralysis can be seen in individuals of all ages, adults and children, with varying level of affect. One of the common cause or frequent occurrences of palsy is due to idiopathic Bell's palsy [2], in adults it is accounted about 54.9% of cases and in children it is 66.2%. One more similar form of palsy is due to a virus called Ramsay Hunt Syndrome [3],[4]. Among adults this is calculated as 26.8% and 14.6% among children. The other leading causes for facial paralysis are Traumas, which are see during childbirth, accidents, surgeries and strokes, these include about 5.9% cases in adults and in children it is 13.4%. Individually, birth traumas account for 3.4%, iatrogenic reasons account for 2%, tumors account for 1,8% in adults and 1.3% from leukemia cases among children. For detecting the key points on the image of patients face a CNN-based model is used with auto encoders in the process. In further study, this can be useful for comparing the symmetry level. The early detection of the facial paralysis is desirable as the treatment in the initial stage will have more chances of recovering faster, since the recovery rate may be diminishing with aging.

II. RELATED WORKS

Kostiantyn Khabarlak, et.al [5], this paper presents a comprehensive overview of traditional and deep learning-based approaches for facial landmark detection. The authors provide a detailed analysis of the strengths and limitations of each approach, along with a comparison of their performance on benchmark datasets. This paper discusses the applications of facial landmark detection, including facial expression recognition, face tracking, and facial reenactment. It provides examples of how these applications are used in various domains such as entertainment, healthcare, and security. This information is critical for researchers who want to address the existing limitations of facial landmark detection methods and develop new approaches to overcome them. There are a few more methods [6] suggested earlier for similar outcomes and This can serve as an excellent starting point for researchers who want to understand the current state-of-the-art in facial landmark detection and identify areas for future research.

Gemma S.Parra-Dominguez et al., This paper [7] is highly relevant to medical imaging and computer vision research, particularly for those working on facial paralysis diagnosis and treatment. In a detailed review of existing methods for facial paralysis detection, including manual inspection by medical professionals, electromyography, and image analysis techniques. The limitations of these methods are particularly in terms of their accuracy, cost, and availability. This information is useful for researchers who want to understand the challenges associated with facial paralysis detection and the need for improved methods. This proposes a new method for facial paralysis detection based on key point analysis. They evaluate the performance of the proposed method using a dataset of facial images and compare it with existing methods.

Samuel Susan Veeravalli et al [8], in this, the suggested technique classifies the dataset of drooping facial photographs by comparing them to the dataset of normal face images. The identification of face pictures with palsy is made possible by the best deep learning image classification methods. The trained models are quite accurate in detecting the same. The three models' comparisons, together with earlier research, show that DenseNet201 has the highest

accuracy for both training and validation. As a result, this method is helpful in identifying people who have facial malformations.

Chaoqun Jiang, et al. [9] provides a comprehensive review of existing methods for facial paralysis assessment, including manual inspection by medical professionals, electromyography, and image analysis techniques. The authors highlight the limitations of these methods, particularly in terms of their accuracy, reliability, and cost. This information is valuable for researchers who want to understand the challenges associated with facial paralysis assessment and the need for improved methods. This show that the proposed method achieves high accuracy in automatic facial paralysis assessment and outperforms existing methods in terms of speed and cost-effectiveness. The paper also discusses the potential applications of the proposed method, including diagnosis, treatment planning, and rehabilitation. The importance of early and accurate detection of facial paralysis and the potential impact of the proposed method on patient outcomes. This provides a valuable contribution to the field of automatic facial paralysis assessment using computational image analysis.

Jocelyn Barbosa, et al, the paper [10] proposes a novel method for efficient facial paralysis classification using an ensemble of regression tree-based facial features extraction. It is highly relevant to medical imaging and computer vision research, particularly for those working on facial paralysis diagnosis and treatment. The paper provides a detailed review of existing methods for facial paralysis classification, including manual inspection by medical professionals, electromyography, and image analysis techniques. This proposes a new method for facial paralysis classification based on an ensemble of regression tree-based facial feature extraction. The authors use a combination of facial landmarks, texture, and symmetry features to extract relevant information from facial images and classify the severity of facial paralysis.

Gee-Sern Jison Hsu et al,[11] provides a comprehensive review of existing methods for facial palsy detection, including manual inspection by medical professionals, electromyography, and image analysis techniques. The paper proposes a new method for facial palsy detection based on a hierarchical network. The authors use a multi-level feature extraction approach to capture both local and global facial features and classify the severity of facial palsy using a convolutional neural network (CNN). The proposed method achieves high accuracy in facial palsy detection and outperforms existing methods in terms of speed and efficiency. The paper can serve as a useful resource for researchers working on facial palsy diagnosis and treatment and can inspire new approaches for improving the accuracy and efficiency of facial palsy detection

The Tele Stroke System (TSS) developed by Chandaliya et al. is an innovative telemedicine system [12] designed to enable remote diagnosis and treatment of stroke patients. The TSS system uses technology to connect healthcare professionals with patients in remote locations, providing timely and accurate stroke diagnosis and treatment. The TSS system includes several features such as video conferencing, electronic health record integration, and imaging tools to enable remote consultation, assessment, and treatment planning. Several studies have been conducted to evaluate the effectiveness of the TSS system. One study by Nelson et al. found that the TSS system enabled timely and accurate stroke diagnosis and treatment, resulting in improved outcomes for stroke patients. Another study by Hess et al [13] found that the TSS system improved stroke care in rural areas by providing access to stroke

specialists and reducing the time to treatment. The TSS system has also been recognized for its potential to address the challenges of stroke care in underserved areas. In a review by Leira et al. [14], the authors highlight the TSS system as an example of a telemedicine system that can improve access to stroke care in remote and underserved areas.

Jong- Wook Kim et al, Human pose estimation system [15] is a computer vision task that involves detecting and tracking the positions of human body joints or key points in images or videos. It has numerous applications, such as human-computer interaction, activity recognition, augmented reality, and sports analysis. MediaPipe Pose is a popular open-source library developed by Google that provides real-time pose estimation capabilities. The library offers pre-trained models and a framework for developers to integrate pose estimation functionality into their applications. Optimization methods in the context of human pose estimation refer to techniques used to refine and improve the accuracy of pose estimation algorithms. These methods typically involve adjusting model parameters, refining joint localization, or incorporating additional information to enhance the estimation results. Optimization can be done through various approaches, such as gradient-based optimization, expectation-maximization algorithms, or incorporating biomechanical constraints. A humanoid model refers to a representation or simulation of the human body in the form of a robot or virtual character. It aims to replicate a human's structure and movement capabilities, typically with articulated limbs and joints. Humanoid models are used in robotics, animation, and virtual reality applications.

III. METHODOLOGY

The images which contain facial paralysis are given as input to the MediaPipe framework, which is a pre-trained model for acquiring the required key points and contours of the face. The MediaPipe tool gives a model for detecting facial landmarks known a “BlazeFace” model, which is efficient in detection of faces in real time that are used in applications developed for devices based on face detection. In this model, after detecting the face this gives a boundary box with coordinates for the face in the image or video, these boxes are further given as input to a model known as “FaceMesh” which is also in the MediaPipe. The following steps are involved in the process of facial landmark detection.

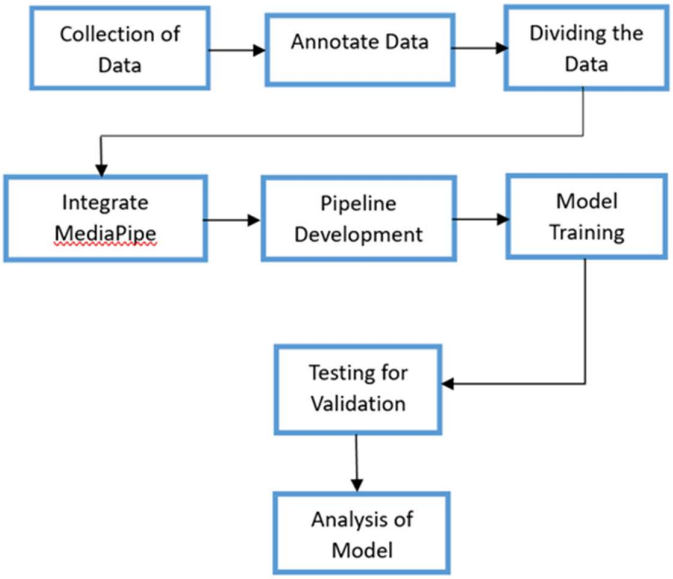

Fig 01: Steps in MediaPipe framework

A. Collection of Data:

This is the initial step for obtaining the dataset containing images or videos of persons who are having notable facial paralysis. It is advisable to have the dataset with the images containing the faces with various range or degree of effect on facial features and also with different expressions.

B. Annotate images:

The dataset that is collected in the previous step is then annotated for the necessary facial landmarks. This can be done using some existing techniques or by manual approach, like FLAT [16], on certain locations like nose edges, Mouth, eyes corners, eyebrow and jawline arcs, etc. The boundary or the shape of these parts are represented using the Contours.

C. Dividing the Data:

The dataset that is annotated is then split into subsets for performing training and testing. The first subset is used to train a model using machine learning algorithms for recognizing the key points and contours. The preprocessing steps are included for data to improve the performance of the model, which are resizing, normalizing and augmentation.

D. Integrate MediaPipe:

In this step, MediaPipe is combined into research pipeline to efficiently grasp the capabilities for identifying the key points and contour of face. The MediaPipe components and certain calculator are incorporated to the pipeline, the components include calculator for detection of face , landmark detection, extraction of contour.

E. Pipeline Development:

The MediaPipe's model that is graph-based is used in developing the pipeline. The available input and output streams are used to select the calculators and are connected, which gives a

completed data processing pipeline. The pipeline should result the necessary key points and contours that are identified by the processing steps on the input images or videos with the use of MediaPipe calculators.

F. Model Training:

The annotated data is used as an input for training the machine learning model, which contain deep learning techniques , where the input images are trained with a neural network to acquire the required key points and contours. The popular frameworks in machine learning like TensorFlow is incorporated in MediaPipe for training and deploying models.

G. Testing for validation:

The second subset of annotated dataset is then used for testing process and validating the developed pipeline. By comparing the obtained key points and contours with the ground true annotations the accuracy and performance are assessed. The performance of the pipeline can also me calculated using the metrics like mean squared error (MSE), Intersection over Union(IoU), accuracy, etc.

H. Analysis of model:

The pipeline which is developed can be used in the experiments involving real -world problems related to facial dissimilarity or paralysis. MediaPipe framework gives a facemesh for the input image resulting in 468 key points in total for the entire face, from these 68 key points for specific facial parts like eyes, nose, mouth, jawline are filtered into separate array. These 68 points are analyzed for further investigations to compare the differences in facial features among individuals who are affected by paralysis and with normal persons, or assessment of different treatments available to reduce the deformation.

RESULTS

In this work, the key points for the given input image are generated. Fig-2 is the input image and the resulting 468 key points are depicted in fig-3, fig-4 shows the necessary 68 key points that are filtered, also the contours for the same are displayed in fig-5. The coordinates for the same are listed in table-1 as shown.

Fig 2: Sample input image containing facial palsy.

Fig 3: Output image with face mesh containing468 Key points

Fig 4: Resulting image after plotting 68 key points.

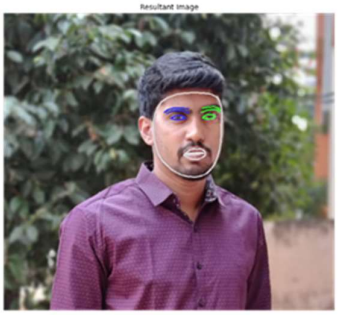

Fig 5: Resulting image with contours for the input.

The values listed in the table denoting the coordinates are with respect to the resolution of the image that is given as input. The original size of the image is 634 x 706 (height to width) pixels. Therefore, the actual value for the x and y coordinate can be multiplied by the size of the image respectively. The values in the table I and II shows the coordinates of the points for right eye and left eye, each of them having six points from one corner to other.

TABLE I: Coordinates for the key points obtained for Right Eye

Facial Part	Key Point	X Coordinate	Y Coordinate	Z Coordinate
Right Eye	R_Eye_point_1	0.506309986114502	0.355097234249115	0.001337579800747335
	R_Eye_point_2	0.5501273274421692	0.35522955656051636	0.0014711711555719376
	R_Eye_point_3	0.5209286212921143	0.3602464497089386	-0.004347117152065039
	R_Eye_point_4	0.536825954914093	0.3593788743019104	-0.004226095508784056

	R_Eye_point_5	0.5336870551109314	0.3461665213108063	-0.006255625281482935
	R_Eye_point_6	0.5175626277923584	0.3483402729034424	-0.006606647279113531

Facial Part	Key Point	X Coordinate	Y Coordinate	Z Coordinate
Left Eye	L_Eye_point_1	0.6393384337425232	0.3497340679168701	0.029469022527337074
	L_Eye_point_2	0.6011586785316467	0.35340988636016846	0.014251863583922386
	L_Eye_point_3	0.628948450088501	0.35633012652397156	0.01922358199954033
	L_Eye_point_4	0.6139788627624512	0.35687071084976196	0.013503559865057468
	L_Eye_point_5	0.6158792972564697	0.34331491589546204	0.011805473826825619
	L_Eye_point_6	0.6311912536621094	0.34374117851257324	0.017339305952191353

TABLE II: Coordinates for the key points obtained for Left Eye

The values in the table III show the respective coordinates for the jawline which contains 17 key points from one side of the jaw staring below the ear to the other side of the jaw below the ear.

TABLE III: Coordinates for the key points obtained for Jawline.

Facial Part	Key Point	X Coordinate	Y Coordinate	Z Coordinate
Jawline	Jaw_point_1	0.4662889242172241	0.47397708892822266	0.0653243213891983
	Jaw_point_2	0.45440709590911865	0.4178914427757263	0.07626544684171677
	Jaw_point_3	0.49300265312194824	0.513913094997406	0.038056567311286926
	Jaw_point_4	0.5586146712303162	0.5520328283309937	0.00827468279749155
	Jaw_point_5	0.5247160792350769	0.5386990308761597	0.01971609890460968
	Jaw_point_6	0.5802183747291565	0.5522043704986572	0.009447998367249966
	Jaw_point_7	0.4563663601875305	0.3413168787956238	0.05318619683384895
	Jaw_point_8	0.4789804220199585	0.4969247877597809	0.05208444595336914
	Jaw_point_9	0.4530186355113983	0.3926563560962677	0.07525524497032166
	Jaw_point_10	0.6518465280532837	0.4622001349925995	0.10358452796936035
	Jaw_point_11	0.6572673320770264	0.4082399904727936	0.11913610249757767
	Jaw_point_12	0.6411159634590149	0.5022811889648438	0.06697291135787964
	Jaw_point_13	0.6000743508338928	0.5481287240982056	0.01574687287211418
	Jaw_point_14	0.6238129138946533	0.5297070741653442	0.03847137466073036
	Jaw_point_15	0.6602292060852051	0.3356098234653473	0.09663072228431702
	Jaw_point_16	0.6466024518013	0.48498111963272095	0.08623723685741425
	Jaw_point_17	0.6575981378555298	0.3844403624534607	0.11939171701669693

The values in the tables IV and V depicts the coordinate values of both left and right eyebrows which contain five key points each, from the edge of the eyebrow from one side to the other.

TABLE IV: Coordinates for the key points obtained for Left Eyebrow

Facial Part	Key Point	X Coordinate	Y Coordinate	Z Coordinate
Right Eyebrow	R_Eyebrow_point_1	0.497997522354126	0.32629138231277466	-0.0128019442781806
	R_Eyebrow_point_2	0.5365955829620361	0.32127827405929565	-0.024188708513975143
	R_Eyebrow_point_3	0.475195974111557	0.3284640908241272	0.015369572676718235
	R_Eyebrow_point_4	0.5153801441192627	0.320792019367218	-0.01945437118411064
	R_Eyebrow_point_5	0.5591016411781311	0.32284578680992126	-0.02472919225692749

TABLE V: Coordinates for the key points obtained for Right Eyebrow

Facial Part	Key Point	X Coordinate	Y Coordinate	Z Coordinate
Left Eyebrow	L_Eyebrow_point_1	0.6487370729446411	0.3202771544456482	0.01745336875319481
	L_Eyebrow_point_2	0.6203615665435791	0.31820231676101685	-0.008039051666855812
	L_Eyebrow_point_3	0.6568631529808044	0.3228420913219452	0.05305963382124901
	L_Eyebrow_point_4	0.6368617415428162	0.3161888122558594	0.004603807348757982
	L_Eyebrow_point_5	0.6008167266845703	0.3215346932411194	-0.016331790015101433

The results displayed in the tables VI and VII shows the coordinate values for the key points that are generated for the facial part Mouth and nose respectively. There are 20 key points for mouth and 9 key points for nose in total.

TABLE VI: Coordinates for the key points obtained for Mouth

Facial Part	Key Point	X Coordinate	Y Coordinate	Z Coordinate
Mouth	Mouth_point_1	0.5841827392578125	0.45975160598754883	-0.02616899274289608
	Mouth_point_2	0.5826618075370789	0.4714776277542114	-0.017498809844255447
	Mouth_point_3	0.5831859111785889	0.47549915313720703	-0.015480970963835716
	Mouth_point_4	0.5834757089614868	0.4926748275756836	-0.01644306257367134
	Mouth_point_5	0.5735774636268616	0.4585569202899933	-0.026789287105202675
	Mouth_point_6	0.5618752837181091	0.46333369612693787	-0.023978769779205322
	Mouth_point_7	0.5452654361724854	0.47858867049217224	-0.0071657029911875725
	Mouth_point_8	0.5496633052825928	0.47635772824287415	-0.008970966562628746
	Mouth_point_9	0.5752015709877014	0.4716854691505432	-0.01836412027478218
	Mouth_point_10	0.5725967884063721	0.4925443232059479	-0.018114721402525902

	Mouth_point_11	0.5747473835945129	0.4757827818393707	-0.016450226306915283
	Mouth_point_12	0.5625845789909363	0.48957252502441406	-0.017323952168226242
	Mouth_point_13	0.5938596129417419	0.45763275027275085	-0.022612666711211205
	Mouth_point_14	0.6026700139045715	0.4613730311393738	-0.015345046296715736
	Mouth_point_15	0.6116791367530823	0.47564616799354553	0.00916778389364481
	Mouth_point_16	0.6068854331970215	0.473694384098053	0.004947157111018896
	Mouth_point_17	0.5888987183570862	0.47108423709869385	-0.01461831945925951
	Mouth_point_18	0.5931878089904785	0.49118345975875854	-0.014190268702805042
	Mouth_point_19	0.5904622077941895	0.47498512268066406	-0.012638097628951073
	Mouth_point_20	0.6011203527450562	0.4872768521308899	-0.009311448782682419

TABLE VII: Coordinates for the key points obtained for Nose.

Facial Part	Key Point	X Coordinate	Y Coordinate	Z Coordinate
Nose	Nose_point_1	0.5840728282928467	0.43312039971351624	-0.024872150272130966
	Nose_point_2	0.5886971950531006	0.41038817167282104	-0.0516398586332798
	Nose_point_3	0.5872846841812134	0.39505475759506226	-0.04807683452963829
	Nose_point_4	0.5635213851928711	0.42742595076560974	-0.02249925769865513
	Nose_point_5	0.5724976062774658	0.4335053265094757	-0.024311047047376633
	Nose_point_6	0.580451250076294	0.3475072383880615	-0.018056349828839302
	Nose_point_7	0.5837765336036682	0.37067151069641113	-0.031630102545022964
	Nose_point_8	0.6013118624687195	0.425798624753952	-0.01617930829524994
	Nose_point_9	0.5943480134010315	0.4327274560928345	-0.020514406263828278

The second sample input for the proposed work is given from the dataset the is available in Kaggle [17] which contains the images of droopy facial images. Fig 6(a) is the input image to generate the facial key points. Fig 6(b), Shows the 68 key points that are identified in this. Fig 6(c) depicts the contours for the image. The resultant values for the key points are tabulated in the Table VIII to Table XIV with X, Y Z coordinates. As the image size is 300 x 215 (height x width) pixels, the respective values can be multiplied for obtaining the coordinates.

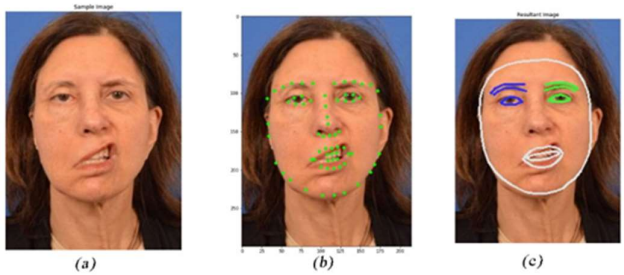

(a) (b) (c)

Fig 6: Sample input and its resultant key points and Contours.

The values in the table VIII and IX shows the coordinates of the points for right eye and left eye, each of them having six points from one corner to other.

TABLE VIII: Coordinates for the key points obtained for Left Eye

Facial Part	Key Point	X Coordinate	Y Coordinate	Z Coordinate
Left Eye	L_Eye_point_1	0.693718	0.356024	0.074992
	L_Eye_point_2	0.566971	0.363759	0.04416
	L_Eye_point_3	0.65796	0.366842	0.045838
	L_Eye_point_4	0.610918	0.369449	0.034641
	L_Eye_point_5	0.612133	0.340777	0.031859
	L_Eye_point_6	0.660384	0.342012	0.042441

TABLE IX: Coordinates for the key points obtained for Right Eye

Facial Part	Key Point	X Coordinate	Y Coordinate	Z Coordinate
Right Eye	R_Eye_point_1	0.27658	0.373302	0.047842
	R_Eye_point_2	0.407993	0.369639	0.031813
	R_Eye_point_3	0.316794	0.382769	0.023291
	R_Eye_point_4	0.365377	0.380383	0.018178
	R_Eye_point_5	0.357511	0.349493	0.015441
	R_Eye_point_6	0.308446	0.354738	0.020106

The values in the tables X and XI depicts the coordinate values of both left and right eyebrows which contain five key points each, from the edge of the eyebrow from one side to the other.

TABLE X: Coordinates for the key points obtained for Left Eyebrow

Facial Part	Key Point	X Coordinate	Y Coordinate	Z Coordinate
Left Eyebrow	L_Eyebrow_point_1	0.710638	0.294792	0.046326
	L_Eyebrow_point_2	0.608602	0.28563	-0.01814
	L_Eyebrow_point_3	0.761126	0.298179	0.152044
	L_Eyebrow_point_4	0.664879	0.28391	0.013566
	L_Eyebrow_point_5	0.546924	0.29083	-0.03647

TABLE XI: Coordinates for the key points obtained for Right Eyebrow

Facial Part	Key Point	X Coordinate	Y Coordinate	Z Coordinate
Right Eyebrow	R_Eyebrow_point_1	0.246274	0.308276	0.018866
	R_Eyebrow_point_2	0.354399	0.290637	-0.0321
	R_Eyebrow_point_3	0.192272	0.324043	0.114259
	R_Eyebrow_point_4	0.293664	0.292903	-0.00762
	R_Eyebrow_point_5	0.419906	0.292245	-0.04287

The values in the table XII show the respective coordinates for the jawline which contains 17 key points from one side of the jaw staring below the ear to the other side of the jaw below the ear.

TABLE XII: Coordinates for the key points obtained for Jawline

Facial Part	Key Point	X Coordinate	Y Coordinate	Z Coordinate
Jawline	Jaw_point_1	0.203752	0.636922	0.226652
	Jaw_point_2	0.161591	0.521391	0.282023
	Jaw_point_3	0.283939	0.712576	0.124541
	Jaw_point_4	0.478703	0.779113	-0.00041
	Jaw_point_5	0.37892	0.755583	0.053353
	Jaw_point_6	0.544595	0.778753	-0.00589
	Jaw_point_7	0.151962	0.359867	0.234551
	Jaw_point_8	0.242303	0.681916	0.176043
	Jaw_point_9	0.153979	0.469216	0.288505
	Jaw_point_10	0.809506	0.59824	0.266553
	Jaw_point_11	0.822868	0.482832	0.326518
	Jaw_point_12	0.758569	0.679109	0.153626
	Jaw_point_13	0.60632	0.769805	0.006101
	Jaw_point_14	0.688064	0.732767	0.071575
	Jaw_point_15	0.800654	0.325586	0.278163
	Jaw_point_16	0.785921	0.64532	0.210978
	Jaw_point_17	0.818119	0.43155	0.333568

The results displayed in the tables XIII and XIV shows the coordinate values for the key points that are generated for the facial part Mouth and nose respectively. There are 20 key points for mouth and 9 key points for nose in total.

TABLE XIII: Coordinates for the key points obtained for Mouth

Facial Part	Key Point	X Coordinate	Y Coordinate	Z Coordinate
Mouth	Mouth_point_1	0.531669	0.57428	-0.09585
	Mouth_point_2	0.533371	0.598879	-0.07276
	Mouth_point_3	0.537453	0.62513	-0.06259
	Mouth_point_4	0.541868	0.66223	-0.06941
	Mouth_point_5	0.494723	0.574477	-0.09369
	Mouth_point_6	0.4593	0.587314	-0.07958
	Mouth_point_7	0.413165	0.625655	-0.01104
	Mouth_point_8	0.430504	0.621356	-0.01877
	Mouth_point_9	0.506039	0.601677	-0.07074
	Mouth_point_10	0.502415	0.663079	-0.06961
	Mouth_point_11	0.50735	0.626873	-0.061
	Mouth_point_12	0.468462	0.656329	-0.0584
	Mouth_point_13	0.565927	0.566909	-0.08901
	Mouth_point_14	0.601543	0.570924	-0.06982
	Mouth_point_15	0.651121	0.597364	0.004219
	Mouth_point_16	0.631645	0.597036	-0.00549
	Mouth_point_17	0.559309	0.595479	-0.0676
	Mouth_point_18	0.578709	0.656122	-0.06526
	Mouth_point_19	0.565832	0.620861	-0.05624
	Mouth_point_20	0.608695	0.642902	-0.04946

TABLE XIV: Coordinates for the key points obtained for Nose

Facial Part	Key Point	X Coordinate	Y Coordinate	Z Coordinate
Nose	Nose_point_1	0.518314	0.519412	-0.08959
	Nose_point_2	0.510557	0.469086	-0.169
	Nose_point_3	0.505048	0.439153	-0.15399
	Nose_point_4	0.453416	0.511546	-0.07293
	Nose_point_5	0.482301	0.523024	-0.08368
	Nose_point_6	0.48887	0.346233	-0.04171
	Nose_point_7	0.496673	0.393138	-0.09342
	Nose_point_8	0.573483	0.500943	-0.06649
	Nose_point_9	0.55226	0.516354	-0.08003

CONCLUSION

In this paper, the need for detecting facial key points is discussed. The framework for generating key points in some applications involving face mesh detection are used. MediaPipe is the framework that provided an accurate key point for images that contain facial palsy. This study further helps in analyzing the degree of asymmetry for facial parts like eyes, mouth and jawline, and thus can be useful for medical diagnosis. The comparison of facial key points during the recovery phase of patients having facial palsy can be done using this. This also facilitates the analysis of recovery time in different causes of palsy and to better understand the treatments that are available.

REFERENCES

[1] GCha CI, Hong CK, Park MS, Yeo SG. Comparison of facial nerve paralysis in adults and children. Yonsei Med J. 2008 Oct 31;49(5):725-34. doi: 10.3349/ymj.2008.49.5.725. PMID: 18972592; PMCID: PMC2615370.

[2] I. Song, N. Y. Yen, J. Vong, J. Diederich, and P. Yellowlees, ‘‘Profiling bell’s palsy based on House-Brackmann score,’’ J. Artif. Intell. Soft Comput. Res., vol. 3, no. 1, pp. 41–50, Dec. 2014.

[3] Sweeney CJ, Gilden DH, “Ramsay Hunt syndrome” Journal of Neurology, Neurosurgery & Psychiatry 2001;71:149-154.

[4] Kanerva, M., Jones, S. & Pitkaranta, A. “Ramsay Hunt syndrome: characteristics and patient self-assessed long-term facial palsy outcome”. Eur Arch Otorhinolaryngol 277, 1235–1245 (2020). https://doi.org/10.1007/s00405-020-05817-y

[5] K. Khabarlak, L. Koriashkina Fast Facial Landmark Detection, and Applications: A Survey. Journal of Computer Science & Technology, vol. 22, no. 1, pp. 12–41, 2022.

[6] Y. Wu and Q. Ji, “Facial landmark detection: A literature survey,” Int. J. Comput. Vision, vol. 127, no. 2, pp. 115–142, Feb. 2019, ISSN: 0920-5691. DOI: 10. 1007/s11263-018-1097-z.

[7] Parra-Dominguez GS, Sanchez-Yanez RE, Garcia-Capulin CH. Facial Paralysis Detection on Images Using Key Point Analysis. Applied Sciences. 2021; 11(5):2435. https://doi.org/10.3390/app11052435

[8] Samuel Susan Veeravalli, Dr. Prajna Bodapati. Deep Learning Approach To Detect Facial Asymmetry For Paralysis Detection. Journal of Theoretical and Applied Information Technology, 2023 June, Vol.101.No.12, E-ISSN:1817-3195

[9] Jiang C, Wu J, Zhong W, Wei M, Tong J, Yu H, Wang L. Automatic Facial Paralysis Assessment via Computational Image Analysis. J Healthc Eng. 2020 Feb 8; 2020:2398542. doi 10.1155/2020/2398542. PMID: 32089812; PMCID: PMC7031725

[10] Barbosa J, Seo WK, Kang J. paraFaceTest: an ensemble of regression tree-based facial features extraction for efficient facial paralysis classification. BMC Med Imaging. 2019 Apr 25;19(1):30. doi 10.1186/s12880-019-0330-8. PMID: 31023253; PMCID: PMC6485055.

[11] G. -S. J. Hsu, W. -F. Huang and J. -H. Kang, "Hierarchical Network for Facial Palsy Detection," 2018 IEEE/CVF Conference on Computer Vision and Pattern Recognition Workshops (CVPRW), 2018, pp. 693-6936, doi: 10.1109/CVPRW.2018.00100.

[12] Chandaliya, Rishabh & Joshi, Praveen & Afli, Haithem. (2021). TeleStroke System (TSS) - Stroke Detection using Machine Learning.

[13] Hess DC, Audebert HJ. The history and future of telestroke. Nat Rev Neurol. 2013 Jun;9(6):340-50. doi: 10.1038/nrneurol.2013.86. Epub 2013 May 7. PMID: 23649102.
[14] Leira EC, Lamb DL, Nugent AS, Ahmed A, Grimsman KJ, Clarke WR, Adams HP Jr. Feasibility of acute clinical trials during aerial interhospital transfer. Stroke. 2006 Oct;37(10):2504-7. doi: 10.1161/01.STR.0000239661.07675.9d. Epub 2006 Aug 31. PMID: 16946166.
[15] Kim, J.-W.; Choi, J.-Y.; Ha, E.-J.; Choi, J.-H. Human Pose Estimation Using MediaPipe Pose and Optimization Method Based on a Humanoid Model. Appl. Sci. 2023, 13, 2700. https://doi.org/10.3390/app13042700.
[16] https://www.cv-foundation.org/openaccess/content_cvpr_workshops_2013/W16/html/Sagonas_A_Semi-automatic_Methodology_2013_CVPR_paper.html
[17] "Facial_Droop_and_Facial_Paralysis_image," Kaggle, 23-Aug-2019. [Online]. Available: https://www.kaggle.com/kaitavmehta/facial-droop-and-facial-paralysis-image. [Accessed: 20-Jan-2022].